

## Low temperature afterglow from SrAl<sub>2</sub>O<sub>4</sub>: Eu, Dy, B containing glass

V. Vitola<sup>a,\*</sup>, V. Lahti<sup>b</sup>, I. Bite<sup>a</sup>, A. Spustaka<sup>a</sup>, D. Millers<sup>a</sup>, M. Lastusaari<sup>c,d</sup>, L. Petit<sup>b</sup>, K. Smits<sup>a</sup>

<sup>a</sup>University of Latvia, Institute of Solid State Physics, Kengaraga 8, Riga, Latvia

<sup>b</sup>Photonics Laboratory, Tampere University, Korkeakoulunkatu 3, 33720, Tampere, Finland

<sup>c</sup>University of Turku, Department of Chemistry, FI-20014 Turku, Finland

<sup>d</sup>Turku University Centre for Materials and Surfaces (MatSurf), Turku, Finland

### ARTICLE INFO

#### Article history:

Received 26 June 2020

Revised 7 August 2020

Accepted 12 August 2020

#### Keywords:

Persistent luminescence

Phosphate glass

Low temperature applications

### ABSTRACT

SrAl<sub>2</sub>O<sub>4</sub>: Eu, Dy, B particles were added in a phosphate glass (90NaPO<sub>3</sub>-10NaF (in mol%)) using the direct doping method. For the first time, the composition of the particles prior to and after embedding them in the glass was analysed using EPMA analysis. Boron was found to be incorporated in already distorted surroundings creating new trapping centers in the particles which are thought to be favourable for the tunnelling process and so for the afterglow at 10K. Despite the partial decomposition of the particles, the glass exhibit afterglow at low temperature confirming to be promising materials for low temperature applications.

© 2020 Acta Materialia Inc. Published by Elsevier Ltd. All rights reserved.

Persistent luminescence is light emission from excited material that can last for several minutes or even hours after the termination of the excitation [1]. Luminescent materials use energy from some external source, such as sunlight for example and store it by the means of localizing charge carriers in some trapping centers. The charge carriers are released gradually from the trapping centers, followed by recombination process and emission of light. SrAl<sub>2</sub>O<sub>4</sub>:Eu,Dy is one of the most efficient persistent luminophores known up-to-date [2, 3]. The afterglow can be observed for up to 20 hours after removing the excitation [1–3]. Due to its strong and extensive afterglow, SrAl<sub>2</sub>O<sub>4</sub>: Eu, Dy luminophore is widely used in many applications – emergency signs, luminous paints, luminescent coatings, in vivo imaging [2–6].

However, luminophores from Eu doped aluminate group lose 90% of their afterglow efficiency in temperatures below zero Celsius, which is a major problem for material outdoor use [7]. Recently it has been observed, that the addition of boron between 5 and 7 at% in SrAl<sub>2</sub>O<sub>4</sub>:Eu,Dy during the synthesis led to particles with afterglow even in temperatures as low as 10K, however the reasoning for this is unclear [8]. As for the other drawback, the PL (persistent luminescent) luminophores are usually obtained during synthesis in the form of non-transparent powders thus limiting the excitation and emission to the surface of the material and therefore wasting the material in the volume. Therefore, a possible solution is to disperse these luminophores in a transparent matrix to increase the intensity of the persistent luminescence emission

by exciting the entire volume of the host optimizing the usage of luminescent microparticles.

Glasses based materials have been successfully prepared with Eu<sup>2+</sup>,Dy<sup>3+</sup>-doped SrAl<sub>2</sub>O<sub>4</sub> using the “Frozen sorbet method” [9] and also using the direct doping method [10]. In the “Frozen sorbet method”, the luminophore precipitates using the elements from the glass and therefore, the composition of the luminophore can not be controlled. On the other hand, persistent luminescent glasses can be prepared independently of their composition using the direct doping method as the luminophore with target composition and spectroscopic properties are added in the glass melt. However, as explained in [10], the direct doping method needs to be optimized as decomposition of the particles occurs during the glass preparation. The decomposition of the particles depends on the temperature at which the particles are added in the melt and also on the duration the particles are in contact with the glass melt. Using optimized doping parameters, phosphate glasses with the composition 90NaPO<sub>3</sub>-10NaF (in mol%) were successfully prepared with persistent luminescence by adding various commercial persistent luminescent particles in the glass melt [11, 12]. This glass was chosen due to its low melting temperature and high capacity for dopant particles. The addition of the promising boron containing SrAl<sub>2</sub>O<sub>4</sub>:Eu,Dy particles in this glass would allow the fabrication of a promising composite for low-temperature sensing applications.

In this paper, we present, for the first time, a glass-based composite that exhibits afterglow at very low temperatures. The morphological and luminescent properties of the luminophores are dis-

\* Corresponding author.

E-mail address: [virginija.vitola@cfi.lu.lv](mailto:virginija.vitola@cfi.lu.lv) (V. Vitola).

cussed, as well as the change in the distribution of the trapping center when embedding the luminophores in the glass.

In the present study, Eu, Dy, and B doped  $\text{SrAl}_2\text{O}_4$  samples were synthesized using the sol-gel method described in [8]. 1 at% Eu, 2 at% Dy  $\text{SrAl}_2\text{O}_4$  samples were prepared with 5 and 7 at% of boron (labelled as 5% B and 7% B, respectively). However, not all the added boron successfully incorporates in the lattice of the microparticles as shown in the XPS analysis in [8] – the resulting samples contain 3.70 and 6.05% of B, respectively. The  $\text{SrAl}_2\text{O}_4$ :Eu, Dy (with 0.05 and 0.07 B addition) particles were then added in the glass with the composition  $90\text{NaPO}_3$ - $10\text{NaF}$  (in mol%) using the direct doping method as in [10]. The glass was prepared using  $\text{Na}_6\text{O}_{18}\text{P}_6$  (Alfa-Aesar, technical grade),  $\text{Na}_2\text{CO}_3$  (Sigma-Aldrich, >99.5%) and NaF (Sigma-Aldrich, 99.99%). After melting the glasses at  $750^\circ\text{C}$ , the temperature of the glass melt was reduced to  $575^\circ\text{C}$  before adding 0.25 weight-% of the PL particles. 3 min after adding the particles, the glasses were quenched and finally annealed at  $40^\circ\text{C}$  below their respective glass transition temperature for 6h in air. The glasses prepared with the particles doped with  $x=0.05$  and 0.07 of boron are labelled 5% glass and 7% glass, respectively.

An Electron Probe MicroAnalyzer (EPMA) (CAMECA, SX100) was used to determine the composition of the glasses and of the particles with an accuracy of  $\pm 0.1$  at % using the Cameca QUANTI-TOOL analytical programme. The EPMA was operated at 15 keV and 40 nA. Prior to the measurement, the samples were polished and coated with a carbon layer to prevent charging.

The persistent luminescence spectra were recorded using Andor Shamrock B303-I spectrometer. The samples were excited by pulsed laser excitation. Excitation source was YAG:Nd laser LCS-DTL-382QT (266 nm, 8 ns). The decay profiles were also recorded using the same equipment. For thermally stimulated luminescence (TSL) measurements, the samples were cooled with Sumitomo HC-4 closed-cycle helium cryostat, temperature range 9 – 325 K. Lake Shore 331 Temperature controller was used for temperature control as well as for sample heating (6 K/min) during TSL measurements up to 320 K. The excitation source for TSL measurements was X-ray tube with W target (30kV, 10 mA), the samples were irradiated for 20 minutes and the measurement was initiated right after the termination of excitation.

$\text{SrAl}_2\text{O}_4$ : Eu, Dy particles with 5% and 7% B addition were chosen in this study due to their excellent afterglow at 10K as reported in [8]. The reader is referred to this paper for a complete characterization of the particles. EPMA was used to analyse the composition of the particles prior to adding them in the glass.

According to the composition analysis (Fig. 1), boron seems to be unevenly distributed throughout the particles. There are some doubts in the scientific community about the role of boron, when it enters the lattice of  $\text{SrAl}_2\text{O}_4$  [13–15]. Boron is believed to create a shrinkage of lattice and a distortion of the  $\text{Dy}^{3+}$  environment, but the thermally stimulated luminescence data are not consistent in between different publications when discussing the trapping centers in the material that are altered due to the introduction of B – one point of view is that boron itself without Dy does not contribute to creation of trapping centers significant for persistent luminescence and the key to long afterglow is the Dy-borate complex [13], however more recent papers talk about boron induced trap levels, that are present even without Dy [14]. The concentration of Al decreases while the concentration of B increases indicating that B is incorporated in the lattice site of Al. Dy follows the same pattern, as visible in compositional analysis (Fig. 1.), leading to the conclusion that B tends to incorporate in close proximity of Dy, confirming the Dy-borate complex creation. Recently it has been discussed that the low temperature luminescence in  $\text{SrAl}_2\text{O}_4$ :Eu, Dy is due to the creation of excited  $\text{Eu}^{2+}$  via direct tunnelling from some trapping centers, that can not be emptied thermally due to lack of thermal energy [16]. One of the possibilities of the

unknown electron trapping centers in  $\text{SrAl}_2\text{O}_4$  luminophores is the Dy – distorted  $\text{AlO}_4$  tetrahedra [3]. If B incorporates instead of Al in the crystal lattice, the smaller ionic size of B leads to distortion of the lattice. Previous research confirmed the existence of substitutional  $\text{BO}_4$  units in the samples when adding boron [14].  $\text{BO}_4$  is more ionic in comparison to  $\text{AlO}_4$  due to the higher electronegativity and smaller size of B compared to Al [14]. Therefore, the B addition presumably would create lattice distortions, that can lead to electron trapping. Dy ions, when incorporating in the Sr lattice site, has an uncompensated charge stimulating the charge trapping on  $\text{BO}_4$  units. The EPMA analysis allow us to conclude, that B incorporates in already distorted surroundings creating new trapping centers in the material which are thought to be favourable for the tunnelling process.

The particles were added in the glasses using the direct doping method. The glasses exhibit homogeneous green PL confirming the survival of well dispersed particles in the glasses. The photoluminescence spectra (Fig. 2a and b) show a broad emission band with maximum at 530 nm, that can be attributed to the  $\text{Eu}^{2+}$  emission band.

The samples were cooled to 10K temperature and the spectra were recorded. Both particles exhibit a narrowing of the emission band due to the lack of phonon interactions and a second peak also emerges at 455 nm. This peak is attributed to  $\text{Eu}^{2+}$  emission from differently coordinated Sr sites and is thermally quenched at temperatures above 150 K as explained in [3]. We can note that the PL spectra measured at RT do not change significantly when incorporating the luminophores in glass matrix: the intensity of the band at 455 nm compared to the main band at 530 nm increases when performing the measurement at 10K, as well as a slight change in the position of the second peak indicating that the site of the RE ions in the particles is slightly changed after embedding the particles in the glass. As explained in [10], the changes in the site of the RE ions can be due to the partial decomposition of the particles occurring during the glass preparation. As depicted in Fig. 3, Al and Sr can be found in the glass at the glass-particles interface confirming the partial decomposition of the particles associated with the diffusion of the elements from the luminophore to the glass.

The average size of the particles found at the surface of the glasses is around  $100 \mu\text{m}$  indicating that the particles have agglomerated in the glass increasing their size and therefore decreasing the surface/volume ratio. The composition analysis reveals that the particles conserved their compositional integrity: they exhibit a quite homogeneous distribution of  $\text{Al}_2\text{O}_3$  and SrO in their center. It should be noted that there are no characteristic  $\text{Eu}^{3+}$  lines visible in the photoluminescence spectra of the glasses. Therefore we can conclude that although  $\text{Eu}^{2+}$  are also suspected to diffuse in the glass, there is no (or little) oxidation from  $\text{Eu}^{2+}$  to  $\text{Eu}^{3+}$  taken place during the melting process.

The PL decay of the particles prior to and after being embedded in the glass are shown in Fig. 4a. The microparticles alone show an afterglow of several hours in room temperature and close to one hour in the low temperature region before they reach the level of 0.32 mcd, as discussed in [8] – the afterglow times do not significantly differ in 5% and 7% B particles. However, when incorporated in glass, the afterglow time is reduced due to the particle degradation during melting procedure (Table 1). What is interesting to note is that the sample with more boron shows a greater afterglow time in 10 K temperature and smaller afterglow time in room temperature. This would serve as a confirmation to the claim that boron addition contributes to energetically deeper trap creation that are in close vicinity to the luminescence center [14], as they are favourable for tunnelling process, but less favourable for thermal release in room temperature.

The TSL analysis of the particles and particles containing glass were carried out in temperature range 10-320K (Fig. 4b). The parti-

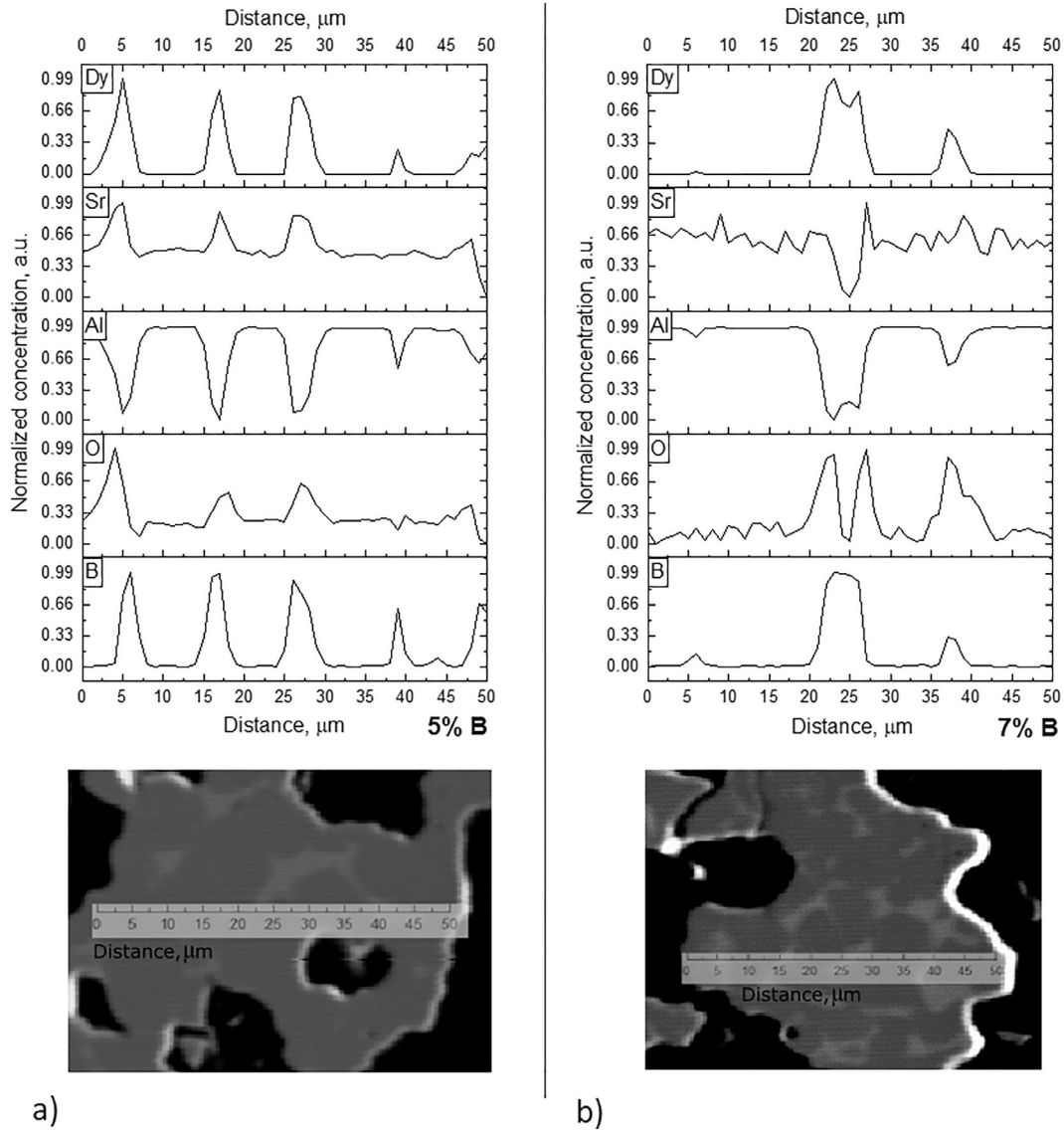


Fig. 1. Composition analysis of the  $\text{SrAl}_2\text{O}_4:\text{Eu, Dy}$  particle with 5% B (a) and 7% B (b).  $\mu$

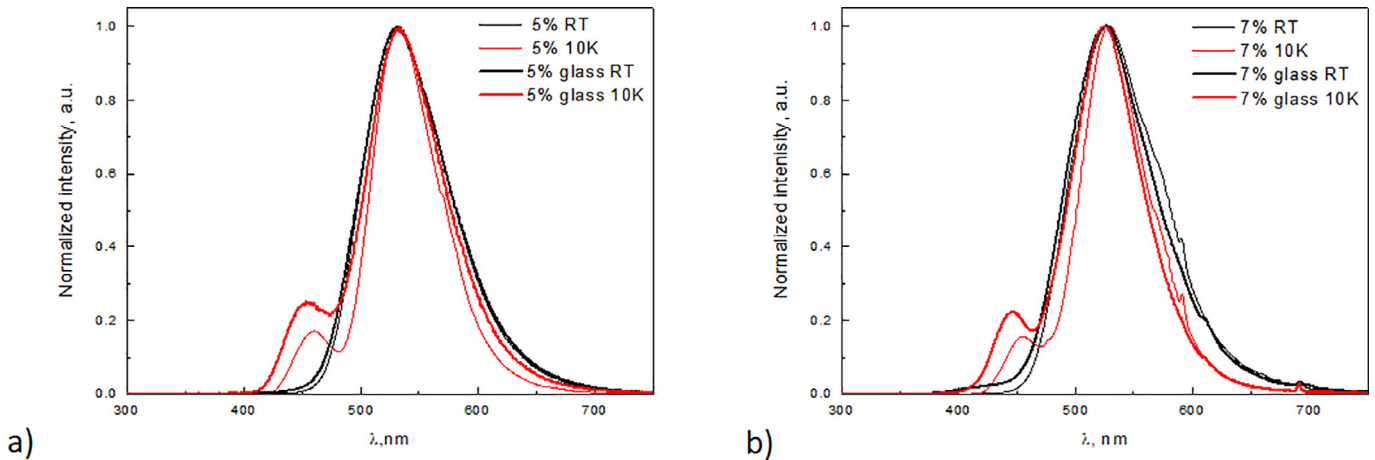


Fig. 2. Photoluminescence spectra of the PL glass and of the PL particles alone with a) 5% B and b) 7% B. The spectra were measured at room temperature and at 10K.

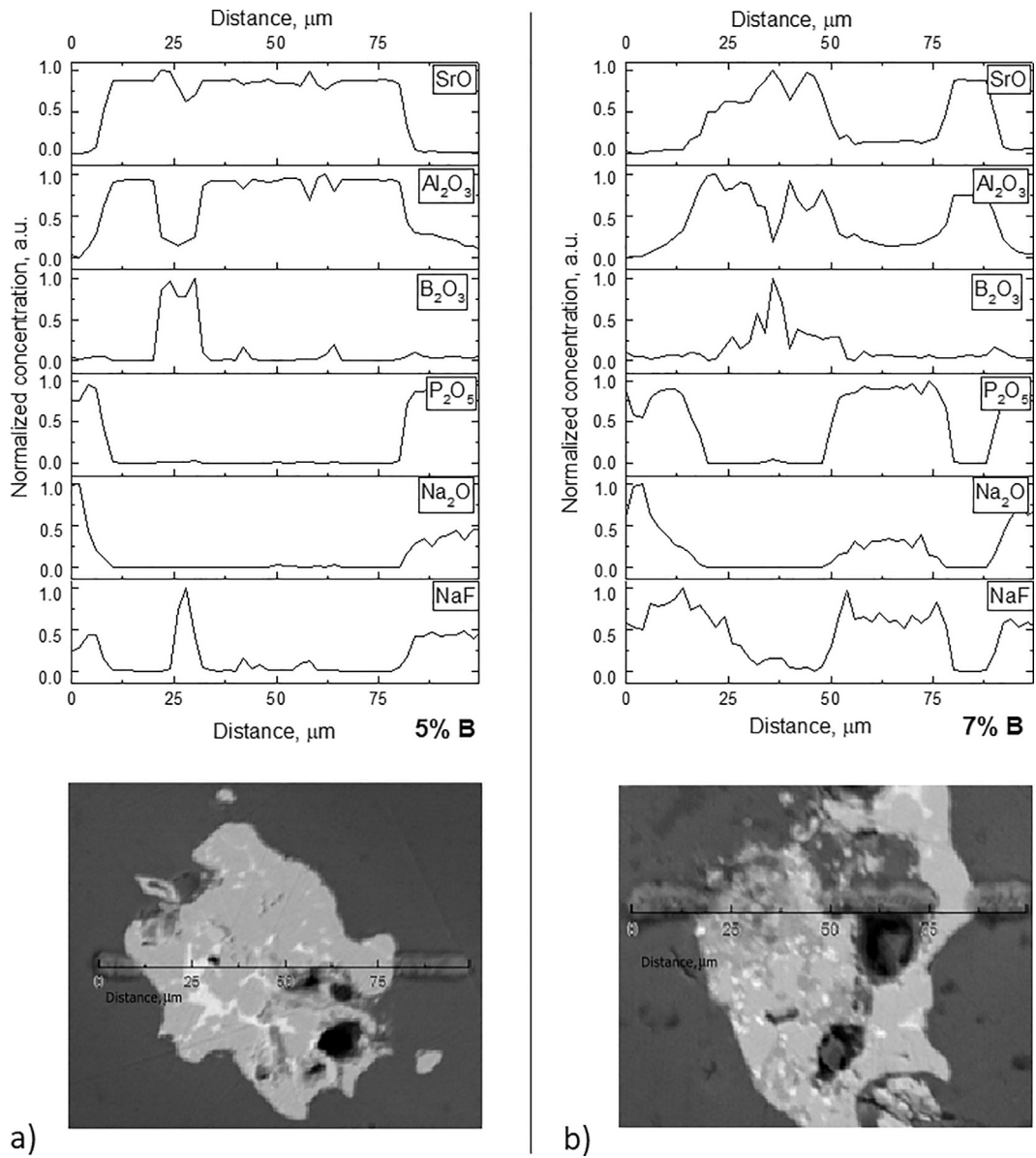


Fig. 3. Composition analysis of the  $\text{SrAl}_{2-x}\text{B}_x\text{O}_4: \text{Eu, Dy}$  particle after embedding in glass with with 5% B (a) and 7% B (b).

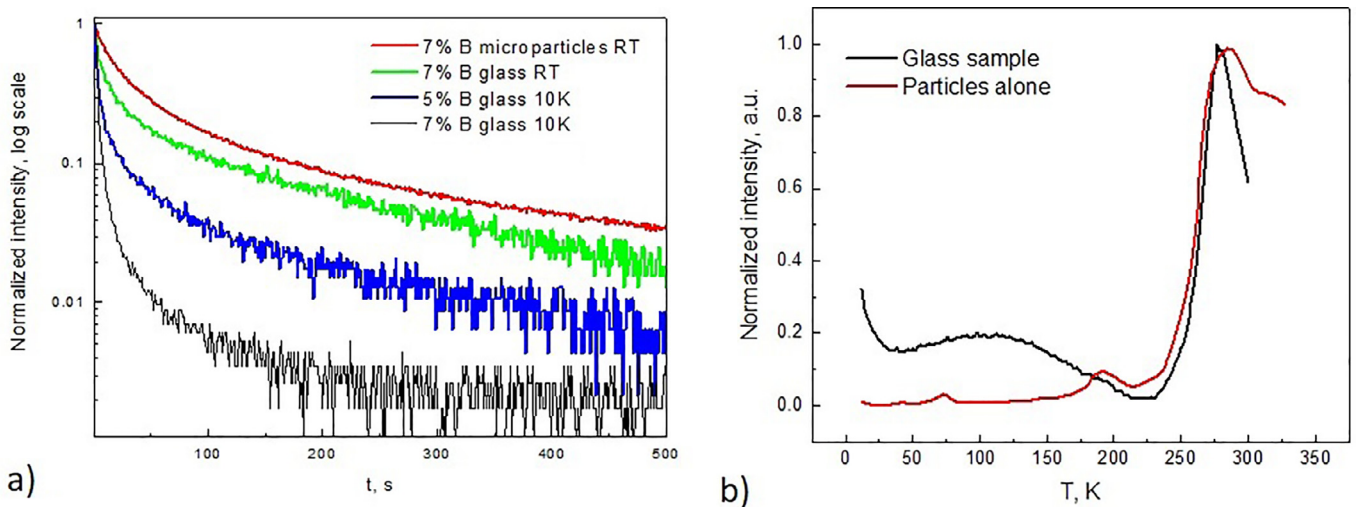


Fig. 4. Photoluminescence decay kinetics comparison of the particles alone and of the glasses (a) and thermally stimulated luminescence (TSL) spectra of the particles with 7% B prior to and after being embedded in the glass (b).



**Table 1**

Afterglow time until reaches 1% of initial intensity of the investigated particles containing glass measured at room temperature (RT) and at 10K.

	5% B		7% B	
	RT	10K	RT	10K
Particles alone	>8 hours	> 50 min	>8 hours	> 50 min
Particles embedded in glass	150 min ± 10s	50 s ± 10s	20 min ± 10s	300 s ± 10s

cles alone exhibit quite distinct TSL peaks which can be related to well-defined trapping center (intrinsic  $\text{SrAl}_2\text{O}_4$  defects as discussed in [17]) energies. However, the wide TSL peak with maximum at around 100K of the particles embedded in the glass is a clear indication that the trapping center energies are spread out after embedding the particles in the glass. The defect concentration in the particles increases when adding the particles in the glass and the defects might migrate with respect to their position in particles due to the partial decomposition of the particles during the glass melting, resulting in a different trapping center distribution.

In summary, phosphate glasses containing  $\text{SrAl}_2\text{O}_4:\text{Eu}^{2+}$ ,  $\text{Dy}^{3+}$  were successfully prepared with persistent luminescence at low temperature by adding the B containing PL particles in the glass melt. From the EPMA analysis of the particles alone, B tends to incorporate in already distorted crystal lattice surroundings in the proximity of those Sr lattice sites, that have been replaced by Dy. The addition of B presumably creates different lattice distortions, that can lead to electron trapping. The afterglow decay of the glasses was considerably lower compared to that of the particles alone due to the decomposition of the particles occurring during the glass preparation. However, due to B in the particles, the glass-based materials exhibit afterglow at low temperature creating possible sensing and biomedical applications.

#### Declaration of Competing Interest

The authors declare that they have no known competing financial interests or personal relationships that could have appeared to influence the work reported in this paper.

#### Funding

V.V. acknowledges the financial support of ERDF PostDoc project No. 1.1.1.2/VIAA/3/19/440 (University of Latvia Institute of

Solid State Physics, Latvia) and LP the Academy of Finland (Flagship Programme, Photonics Research and Innovation PREIN-320165 and Academy Project -326418) for the financial support.

Institute of Solid State Physics, University of Latvia as the Center of Excellence has received funding from the European Union's Horizon 2020 Framework Programme H2020-WIDESPREAD-01-2016-2017-TeamingPhase2 under grant agreement No. 739508, project CAMART<sup>2</sup>.

#### References

- [1] J. Xu, S. Tanabe, J. Lumin. 205 (2019) 581–620.
- [2] K. Van den Eeckhout, P.F. Smet, D. Poelman, Mater. 3 (2010) 2536–2566.
- [3] V. Vitola, D. Millers, I. Bite, K. Smits, A. Spustaka, Mater. Sci. Technol. (2019) 1–17.
- [4] I. Bite, G. Kriekle, A. Zolotarjovs, K. Laganovska, V. Liepina, K. Smits, K. Auzins, L. Grigorjeva, D. Millers, L. Skuja, Mater. Des. 160 (2018) 794–802.
- [5] M. Sun, Z. Li, C. Liu, H. Fu, J. Shen, H. Zhang, J. Lumin. 145 (2013) 838–842.
- [6] B. Viana, C. Richard, V. Castaing, E. Glais, M. Pellerin, J. Liu, and C. Chanéac, Springer, Cham. (2020), 163–197
- [7] J. Botterman, P.F. Smet, Opt. Express 23 (2015) A868–A881.
- [8] V. Vitola, I. Bite, D. Millers, A. Zolotarjovs, K. Laganovska, K. Smits, A. Spustaka, Ceram. Int. (2020).
- [9] T. Nakanishi, S. Tanabe, Phys. Status Solidi A 206 (2009) 919–922.
- [10] N. Ojha, H. Nguyen, T. Laihininen, T. Salminen, M. Lastusaari, L. Petit, Corros. Sci. 135 (2018) 207–214.
- [11] N. Ohja, M. Tuomisto, M. Lastusaari, L. Petit, Opt. Mater. (Amst). 87 (2019) 151–156.
- [12] N. Ohja, T. Laihininen, M. Salminen, M. Lastusaari, L. Petit, Ceram. Int 44 (2018) 11807–11811.
- [13] T.R.N.Kutty A.Nag, J. Alloys Compd 354 (2003) 221–231.
- [14] J. Bierwagen, T. Delgado, G. Jiranek, S. Yoon, N. Gartmann, B. Walfort, M. Pollnau, H. Hagemann, J. Lumin. 222 (2020).
- [15] T. Delgado, S. Ajoubipour, J. Afshani, S. Yoon, B. Walfort, H. Hagemann, Opt. Mater. 89 (2019) 268–275.
- [16] V. Liepina, D. Millers, K. Smits, J. Lumin 185 (2017) 151–154.
- [17] V. Vitola, D. Millers, K. Smits, I. Bite, A. Zolotarjovs, Opt. Mater. 87 (2019) 48–52.